

Regulation of peatland evaporation following wildfire; the complex control of soil tension under dynamic evaporation demand

Kettridge, Nicholas; Lukenbach, Maxwell C.; Hokanson, Kelly J.; Devito, Kevin J.; Petrone, Richard M.; Mendoza, Carl A.; Waddington, James Michael

DOI:

[10.1002/hyp.14132](https://doi.org/10.1002/hyp.14132)

License:

Creative Commons: Attribution-NonCommercial (CC BY-NC)

Document Version

Publisher's PDF, also known as Version of record

Citation for published version (Harvard):

Kettridge, N, Lukenbach, MC, Hokanson, KJ, Devito, KJ, Petrone, RM, Mendoza, CA & Waddington, JM 2021, 'Regulation of peatland evaporation following wildfire; the complex control of soil tension under dynamic evaporation demand', *Hydrological Processes*, vol. 35, no. 4, e14132. <https://doi.org/10.1002/hyp.14132>

[Link to publication on Research at Birmingham portal](#)

General rights

Unless a licence is specified above, all rights (including copyright and moral rights) in this document are retained by the authors and/or the copyright holders. The express permission of the copyright holder must be obtained for any use of this material other than for purposes permitted by law.

- Users may freely distribute the URL that is used to identify this publication.
- Users may download and/or print one copy of the publication from the University of Birmingham research portal for the purpose of private study or non-commercial research.
- User may use extracts from the document in line with the concept of 'fair dealing' under the Copyright, Designs and Patents Act 1988 (?)
- Users may not further distribute the material nor use it for the purposes of commercial gain.

Where a licence is displayed above, please note the terms and conditions of the licence govern your use of this document.

When citing, please reference the published version.

Take down policy




While the University of Birmingham exercises care and attention in making items available there are rare occasions when an item has been uploaded in error or has been deemed to be commercially or otherwise sensitive.

If you believe that this is the case for this document, please contact UBIRA@lists.bham.ac.uk providing details and we will remove access to the work immediately and investigate.

RESEARCH ARTICLE

WILEY

Regulation of peatland evaporation following wildfire; the complex control of soil tension under dynamic evaporation demand

Nicholas Kettridge^{1,2}  | Maxwell C. Lukenbach^{3,4} | Kelly J. Hokanson^{3,4} |
 Kevin J. Devito²  | Richard M. Petrone⁵ | Carl A. Mendoza⁴  |
 James Michael Waddington³

¹School of Geography, Earth and Environmental Sciences, University of Birmingham, Birmingham, UK

²Department of Biological Sciences, University of Alberta, Edmonton, Alberta, Canada

³School of Earth, Environment and Society, McMaster University, Hamilton, Ontario, Canada

⁴Department of Earth and Atmospheric Sciences, University of Alberta, Edmonton, Alberta, Canada

⁵Department of Geography and Environmental Management, University of Waterloo, Waterloo, Ontario, Canada

Correspondence

Nicholas Kettridge, School of Geography,
 Earth and Environmental Sciences, University
 of Birmingham, Edgbaston, Birmingham B15
 2TT, UK.

Email: n.kettridge@bham.ac.uk

Funding information

Natural Sciences and Engineering Research
 Council of Canada, Grant/Award Number:
 NSERC-CRDPJ477235-14; Syncrude Canada
 Ltd & Canadian Natural Resources Ltd, Grant/
 Award Number: SCL4600100599

Abstract

The capability of peatland ecosystems to regulate evapotranspiration (ET) following wildfire is a key control on the resilience of their globally important carbon stocks under future climatic conditions. Evaporation dominates post-fire ET, with canopy and sub-canopy removal restricting transpiration and increasing evaporation potential. Therefore, in order to project the hydrology and associated stability of peatlands to a diverse range of post-fire weather conditions and future climates the regulation of evaporation must be accurately parameterised in peatland ecohydrological models. To achieve this, we measure the surface resistance (r_s) to evaporation over the growing season one year post-fire within four zones of a boreal peatland that burned to differing depths, relating r_s to near surface soil tensions. We show that the magnitude and temporal variability in r_s varies with burn severity. At the peatland scale, r_s and near-surface tension correlates non-linearly. However, at the point scale no relationship was evident between temporal variations in r_s and near-surface tension across all burn severities; in part due to the limited fluctuation in near-surface tensions and the precision of r_s measurements. Where automated measurements enabled averaging of errors, the relationship between near-surface tension and r_s switched between periods of strong and weak correlation within a burned peat hummock. This relationship, when strong, deviated from that obtained under steady state laboratory conditions; increases in r_s were more sensitive to fluctuations in near-surface tension under dynamic field conditions. Calculating soil vapour densities directly from near-surface tensions is shown to require calibration between peat types and provides little if any benefit beyond the derivation of empirical relationships between r_s and

This is an open access article under the terms of the Creative Commons Attribution-NonCommercial License, which permits use, distribution and reproduction in any medium, provided the original work is properly cited and is not used for commercial purposes.

© 2021 The Authors. *Hydrological Processes* published by John Wiley & Sons Ltd.

measured soil tension. Thus, we demonstrate important spatiotemporal fluctuations in post-fire r_s that will be key to regulating post-fire peatland hydrology, but highlight the complex challenges in effectively parameterising this important underlying control of near-surface tensions within hydrological simulations.

KEYWORDS

evapotranspiration, fire, negative feedbacks, vadose zone, water repellency, wetland

1 | INTRODUCTION

Peatlands are a key global carbon store, having accumulated ~500 Gt of carbon over millennia (Yu, 2012). They also represent a critical water resource (Holden, 2005), providing the primary landscape water source within the sub-humid climate of the Boreal Plains (Brown et al., 2014; Devito et al., 2017; Gibson et al., 2010). Peatland ecosystems are facing a range of concurrent climate-mediated and land-use change disturbances (Turetsky et al., 2002). These disturbances have the potential to exceed the ecohydrological resilience of northern peatlands (Kettridge et al., 2015) and impact the wider ecohydrological function of the Boreal Plains landscape (Devito et al., 2017; Hokanson et al., 2020). However, peatlands are characterized by an array of negative ecohydrological feedbacks that maintain their characteristic cool and waterlogged conditions, and promote their recovery following disturbance (Belyea & Baird, 2006; Waddington et al., 2015). Evapotranspiration (ET) provides the primary water loss mechanism from these ecosystems within the western Boreal Plains (Brown et al., 2010; Thompson et al., 2015). As such, determining the ecohydrological feedback response of ET to changing climates (Helbig et al., 2020) and disturbances (Bond-Lamberty et al., 2009) is critical to project the future stability and persistence of Boreal Plains peatlands and the associated landscape.

Wildfire represents the largest disturbance to boreal peatlands (Turetsky et al., 2002) and may represent a core catalyst for ecological shifts across the Boreal Plains (Kettridge et al., 2015; Schneider et al., 2016). Wildfire increases potential evaporation by removing the tree and shrub canopies, increasing both the available energy for evaporation (Kettridge et al., 2013) and the connectivity between the atmosphere and evaporating surface (Petrone et al., 2007; Plach et al., 2016). Such increases in PET result in increased evaporation within *Sphagnum* dominated peatlands (Thompson et al., 2014) and, as a result, small increases or decreases in evapotranspiration because of concurrent reductions in transpiration (Morison et al., 2019; Thompson et al., 2014). In comparison, in feather moss dominated peatlands, evaporation can decrease substantially in low severity burns (Kettridge et al., 2017) as a result of increased peat water repellency (Kettridge et al., 2013; Moore et al., 2017); although, this feedback can be exceeded within severe wildfires (Kettridge et al., 2019).

Current studies define the general magnitude and direction of the peatland evaporation feedback following wildfire. However, if we are to represent the absolute response of peatland evaporation to such disturbances under a range of post-fire weather conditions (i.e., both

under current inter-annual weather patterns or future climatic conditions), and to embed this evaporation feedback within the wider network of peatland ecohydrological feedbacks that regulate peatland hydrology (Waddington et al., 2015), it is critical that the mechanistic controls on peatland evaporation are accurately parameterised and incorporated into peatland ecohydrological models (e.g., Moore & Waddington, 2015; Nijp et al., 2017; Sonnentag et al., 2008). Within such models, peatland evaporation is simulated through varying derivations of the Penman–Monteith equation, that at their centre can be simplified to a modified form of the Dalton equation (Oke, 1987):

$$E = \frac{(\rho_{vs}^* - \rho_{va})}{r_s + r_a}, \quad (1)$$

where ρ_{vs}^* is the saturation vapour density of the peat surface, ρ_{va} the vapour density of the air, and r_s and r_a are the surface and aerodynamic resistance, respectively. While the drivers of evaporation [the numerator of Equation (1)] can be obtained from widely available data, uncertainty in the resistances, and notably the surface resistance that regulates the rate of water loss under drying conditions, limits confidence in projections of peatland hydrodynamics under future extremes (Nijp et al., 2017). The surface resistance accounts for the hydration state of the surface (Lehmann et al., 2018) that can be represented by the near surface tensions. Near-surface tension provides a clear indication of this state and strong correlations between peat near-surface tension and r_s have been demonstrated in peat in the laboratory under steady state conditions; evaporation demand held constant (Kettridge & Waddington, 2014). However, it is unclear the extent to which such laboratory based relationships hold under dynamic field conditions; whether (1) the strength of the feedback response under field conditions differs from that of the laboratory-based steady state conditions, (2) strong diurnal fluctuations in evaporative demand and episodic rainfall events in the field induce complex spatiotemporal dynamics in observed relationships, and (3) the formation of water repellent peat that provides a diffusion barrier to water transfer within the near surface (Kettridge et al., 2017; Wilkinson et al., 2020) modifies the previously observed relationships.

The surface resistance provides one approach to incorporate the negative feedback regulation of soil water potential on evaporation in the Penman–Monteith equation. Alternatively, if r_s is assumed to primarily represent the effective reduction in vapour density of the near surface below saturated conditions, evaporation can instead be determined from the difference between in the *actual* vapour density of the peat surface (ρ_{vs}) and the vapour density of the air:

$$E = \frac{(\rho_{vs} - \rho_{va})}{r_a} \quad (2)$$

Under steady state conditions ρ_{vs} can be calculated from near surface tensions providing a direct incorporation of soil tensions within Equation (1):

$$\rho_{vs} = \rho_{vs}^* e^{\left(\frac{\psi M_w g e_c}{R(T + 273.15)}\right)}, \quad (3)$$

where ψ is the soil water potential in the near surface peat, M_w is the molecular weight of water, g is the gravimetric constant, R is the gas constant and T is the surface temperature ($^{\circ}\text{C}$) (Philip, 1957). e_c is an empirical coefficient that corrects for the difference in soil moisture potential between the near-surface (measurement or simulation node) and the soil surface (Alvenäs & Jansson, 1997); when equal to one the surface is in equilibrium with the near-surface pore water pressure:

$$e_c = 10^{-\delta_s \varphi_g}, \quad (4)$$

where φ_g accounts for the difference in tension and δ_s accounts for the temporal variation within this correction factor. Previously δ_s has been assumed to range between -2 and 1 mm and is determined from a simple water balance of the peat surface (Kellner, 2001), with water supply by rainfall, and water loss by evaporation and vapour transfer within the soil. Steady state laboratory based methods (Kettridge & Waddington, 2014) have demonstrated values of e_c to be consistent with both those originally derived for sand (Alvenäs & Jansson, 1997) and applied within model simulations for peatlands (Kellner, 2001). However, the approach has not been directly assessed under dynamic field conditions within peatlands with variations in e_c , notably for periods following rainfall where variations in e_c will be attributed to changes in δ_s .

The aim of this research is to determine the potential of peatland hydrological models to represent the negative feedback response of evaporation to drying of burnt peatlands under dynamic natural environmental conditions. We will: (1) quantify surface resistance to evaporation within a peatland under a range of burn severities, and define its temporal variability in response to diurnal fluctuations in evaporation demand and episodic rainfall events; (2) determine the nature and strength of the relationship between the surface resistance and near-surface tensions under different burn severities, and identify how this differs from steady state laboratory conditions; and (3) quantify the magnitude of the equilibrium coefficient e_c for different peat burn severities, its consistency with laboratory based estimations of its value, and its response to rainfall events.

2 | METHODOLOGY

2.1 | Study site

Measurements were conducted within the Utikuma Region Study Area (URSA) in north-central Alberta (56.107°N 115.561°W), within a

coarse-textured outwash (Devito et al., 2012; Hokanson et al., 2019). Measurements were undertaken within a small peatland lobe approximately 60 m by 150 m in size, surrounded by aspen forestland (cf. Lukenbach, Hokanson, et al., 2015; Figure 1). The peatland was burnt in May 2011 as part of the ~ 90 000 ha Utikuma Complex wildfire (SWF-060). Prior to the fire, the peatland was characterized by feather moss (*Pleurozium schreberi*) lawns underlying a vascular vegetation cover of *Rhododendron groenlandicum* and *Rubus chamaemorus*, and a dense black spruce tree (*Picea mariana*) canopy (~ 7000 stems per hectare). Within the middle area of the peatland *Sphagnum fuscum* hummocks were interspersed within the feather moss lawns. Depth of burn varied between 0.00 to 1.10 m across the site (Lukenbach, Hokanson, et al., 2015). Following the wildfire the site was classified into two zones (middle and margin) determined both from the distance to the pre-fire peatland-upland interface and the burn severity; higher burn severity within the margin peat (burn depth averaging 0.08 ± 0.01 m and 0.42 ± 0.02 m within the middle and margin peat, respectively; cf. Lukenbach, Hokanson et al. (2015)). The peatland middle was further classified into two zones: hummocks (*S. fuscum*) and lawns (feather moss). Lawns accounted for approximately two-thirds of this central zone (cf. Lukenbach, Hokanson, et al., 2015). The margin was covered only by feather moss pre-fire and was again further classified into two zones: areas that had severely burned to mineral soil or areas in which a peat layer remained. This resulted in four classified zones: middle hummocks, middle lawns, margin peat, margin mineral. The water-table depth differed between these four zones of the peatland, averaging 0.65 m (middle hummocks), 0.41 m (middle lawns), 0.18 m (margin peat), and 0.10 m (margin mineral).

2.2 | Hydrological and micrometeorological measurements

ET under defined aerodynamics conditions (within an enclosed chamber, with air mixed by a fan) was measured every hour in each of the designated zones of the peatland throughout the 2012 growing season (May 24th to August 11th), approximately one year following wildfire. Measurements were conducted using an automated version of the chamber approach of McLeod et al. (2004). Three Perspex chambers, with 0.2 m² surface area, were installed within each designated zone. To measure ET, the chamber was closed for 2 min and the air within the chamber continuously mixed by a fan. ET was calculated from the rate of increase in humidity within the closed chamber of known volume (see Kettridge & Waddington, 2014), which was measured using an infra-red gas analyser (Li-COR LI-840). The rate of increase in humidity was determined by fitting a log linear relationship to the humidity difference (difference between the time varying chamber humidity and the constant maximum measured humidity during a given chamber measurement) against time over the first 30 s of each chamber measurement. This log linear relationship was solved to determine the gradient at time zero. Within the low humidity continental climate of the boreal plain, we did not observe extensive fogging within the chamber during the key daytime measurements, and

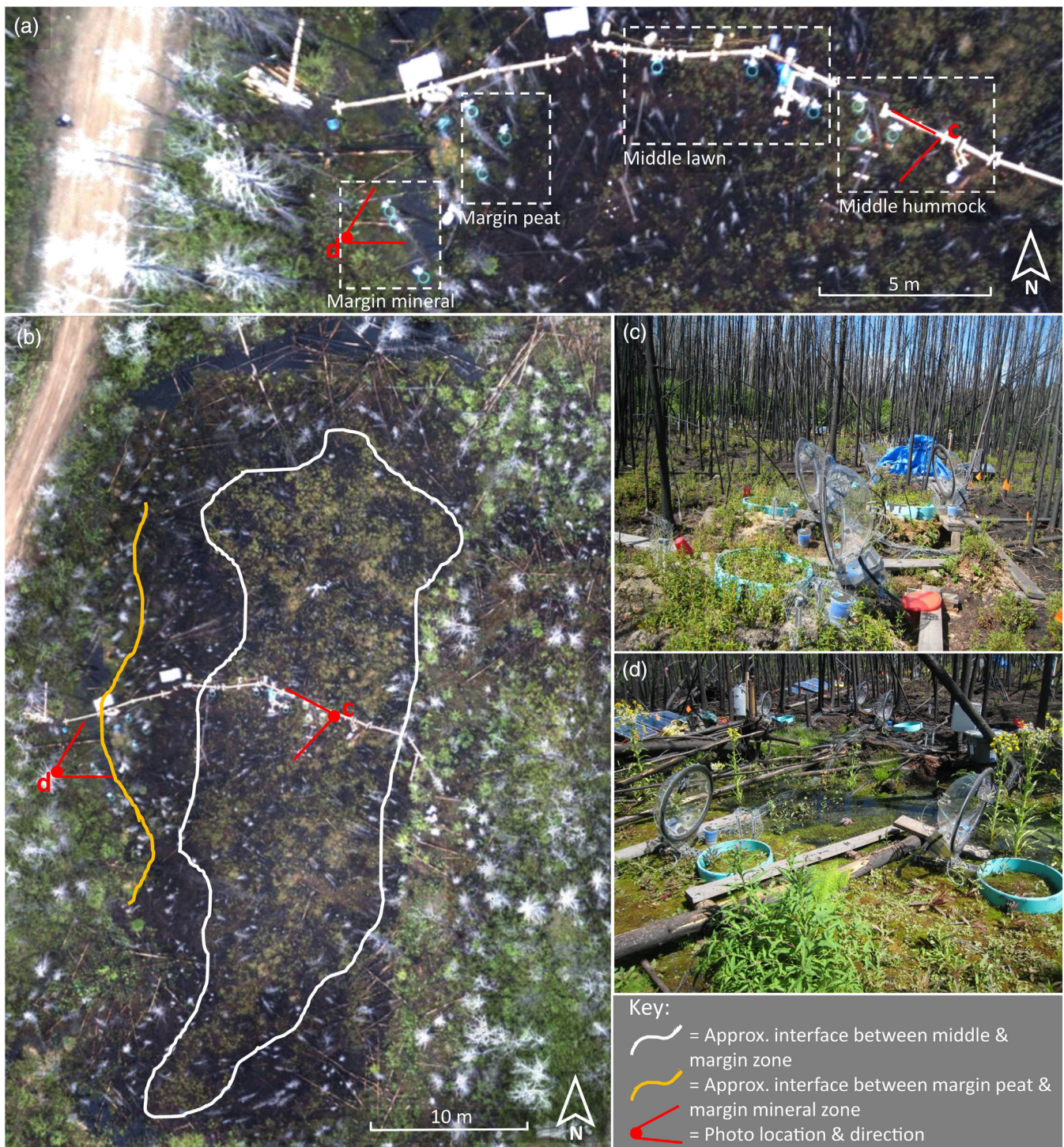


FIGURE 1 Images of the study site. (a) and (b) Photogrammetry (RGB) of the study site from a UAV flown in May 2013. The location of the clusters of chambers within the four zones of the peatland (margin mineral, margin peat, middle lawn, middle hummock) are marked in (a) by dotted white boxes. The exact location of the three turquoise chambers within each of the four zones is visible within the image. (b) Reduced scale showing the entire lobe of the studied peatland, with the approximate interface between the middle and margin zone marked in white, and the approximate interface between the margin peat and margin mineral marked in yellow; the latter in the area of the peatland in which the chambers were installed. The red symbols and associated letter for reference mark the location and direction of the photos taken within the (c) middle and (d) margin of the peatland

notably during the early section of the measurement period used for determination of ET. As a result we did not implement a correction factor to take account of this potential sink function within the

chamber. Such a constant will influence only the absolute magnitude ET measured and not the relative differences between the chambers and over time which is the focus of this study.

In addition to the ET measurements, peat surface temperatures and air temperatures were measured inside each chamber using type T and type K thermocouples, respectively. Surface temperatures were further supplemented with manual infra-red skin surface temperatures obtained within each chamber throughout the growing season using a FLIR i3 infrared camera. The total resistance to ET (r_{total} ; the sum of the surface resistance and aerodynamic resistance) was calculated for each measurement through the inversion of Equation (1) using measurements of surface and air temperature obtained at the point of chamber closure. In laboratory measurements r_a was calculated to equal 62 s m^{-1} by measuring r_{total} for a peat surface that was saturated to minimize r_s to be close to zero (Kettridge et al., 2017). However, it is recognized that r_a may change both in space and time as a result of variations in surface roughness and boundary layer conditions. Throughout, we therefore present the total resistance to evaporation, with the assumption that changes in r_{total} are dominated by variations in r_s .

The leaf area index (LAI) was determined from the inspection of detailed images taken of the chambers through the growing season, using either the leaf count approach (Strack et al., 2004) or image classification in accordance with Kettridge and Baird (2008) depending on the density or type of vegetation. Vascular vegetation was dominated by *R. groenlandicum* with some *R. chamaemorus* in the middle hummocks and by *Epilobium angustifolium* in the margin peat and mineral zones (Figures S1 and S2). Vascular vegetation was not present within the middle lawns. Stomatal conductance was determined for each dominant species within each chamber. Measurements were performed on three leaves, of three separate plants (where possible), within each chamber using an AP4 Delta-T porometer. Within subsequent calculations we apply lower stomatal conductance of *R. groenlandicum* to provide a conservative estimate of the proportion of ET associated with evaporation. In combination with the measured LAI, these measurements were used to estimate the proportion of ET lost via evaporation (cf. Kettridge et al., 2017) assuming a parallel surface and stomatal resistance that act in series with a single aerodynamics resistance.

Based on these assumptions, evaporation varied in its contribution to ET both between zones and through the growing season (Figure S3) resulting both from the variation in resistance of the moss evaporating surface and increases in LAI during the growing season (Figures S1 and S2). At the end of the growing season, evaporation accounted for between 45 and 75% within the middle hummocks and 100% of ET within the middle lawn zone. Within the peat margin and mineral margin, evaporation accounted on average between for 90% to 97% and 89% to 96% of ET, primarily resulting from the low LAI in the first year post fire. As a result, E is assumed to dominate ET across the majority of chambers and, with a big leaf conceptualisation (Admiral & Lafleur, 2007), soil hydrology is assumed to provide the dominant control on r_s . However, the impact of transpiration and the control of stomatal conductance must be borne in mind in the interpretation of the subsequent results. This is notable within Chamber 2 within the middle hummocks where the higher LAI and the higher surface resistance of the moss surface combine so that transpiration

and evaporation are approximately equivalent through the centre of the growing season.

Soil tension was measured adjacent to each chamber within the middle hummocks, margin peat and margin mineral zones at a depth of 0.05 and 0.15 m. Within the middle lawns tensions were not measured directly adjacent to the each chamber, but instead at the same depths at three separate locations in the vicinity of the cluster of chambers. Tensiometers (0.02 m outside diameter; Soil Measurement Systems, Tucson, AZ, USA) were installed and measured manually two to three times per week from May 2012 to August 2012 with a UMS infield tensiometer (Munich, Germany; accuracy ± 0.02 m). Further, diurnal variations in tension were determined during an intensive measurement period in which tensions were measured every 30 min over a 24-h period between 13:00 on day of year 164 to 13:00 on day of year 165, 2012. Only ~ 5 mm of rainfall was measured in the 5 days preceding the measurement period, with the last rainfall event (1.5 mm) occurring 30 h prior to the initiation of measurements. The maximum and minimum temperatures during the measurement period were 26.5 and 8.2°C, respectively. During the daytime, conditions were sunny and a wind speed of ~ 1 m/s was consistently measured, while nighttime hours were characterized by clear and calmer conditions (wind speed generally < 0.5 m/s). These manual measurements were supplemented with two logging versions of the above tensiometers installed within a *S. fuscum* hummock used for chamber measurements (Chamber 2). Tensions were recorded at 20-min intervals for three months during the study period, through May to August. Automatic tensions correlate strongly with manual measurements of these tensiometers ($R^2 > 0.95$, $n = 32$, $p < 0.001$). Logging tensions show consistent patterns between each probe over the measurement period (Figure S4). However, tensiometer 1 better detects the higher tensions during the dry periods of the study (Figure S4) and is applied within the subsequent analysis.

Water table position was recorded at 20-min intervals by capacitance water level recorders (Odyssey Data Recording, Christchurch, New Zealand) that were installed within 0.05 m diameter PolyVinyl Chloride (PVC) wells, one in the middle and one in the margin of the peatland. The depth to water table at locations where the chambers and tensiometers were installed was determined by measuring the water level in the closest well and assuming a flat water table position between the well and the adjacent chamber or tensiometer.

2.3 | Hydrological and micrometeorological analysis

The control of the different measurement zones (middle hummocks, middle lawns, margin peat, margin mineral) on $\log r_{total}$ were analysed using a general linear model in R with zone as a fixed effect and collar ID as a random effect to account for the lack of independence among collar measurements. To quantify the control of water availability on ET, individual measurements of near-surface tension and r_{total} were directly correlated. Further, the diurnal variations in near-surface

tensions observed during the intensive measurement period were related to average diurnal variations in r_{total} observed during the entire study period. The latter approach is applied to average errors in individual r_{total} measurements; errors in measured r_{total} particularly result from small-scale spatial variations in surface temperatures and errors in measured rates of ET (notably under periods of low ET). Such errors under dynamic field conditions could be larger compared to steady state laboratory conditions where solar heating was kept to a minimum (Kettridge & Waddington, 2014).

e_c was calculated for each point in time and space where both a measurement of near surface tension and ET were available. As a result, ET was determined at a low temporal interval across each of the surface chamber measurements and at a high temporal frequency for Chamber 2 in the middle hummock zone, utilizing the logging tensiometer measurements. To calculate e_c we apply a form of Equation (2) to the effective humidity gradient between ρ_{vs}^* , the saturation vapour density of the peat surface, and ρ_{vs} , the actual vapour density of the peat surface, where:

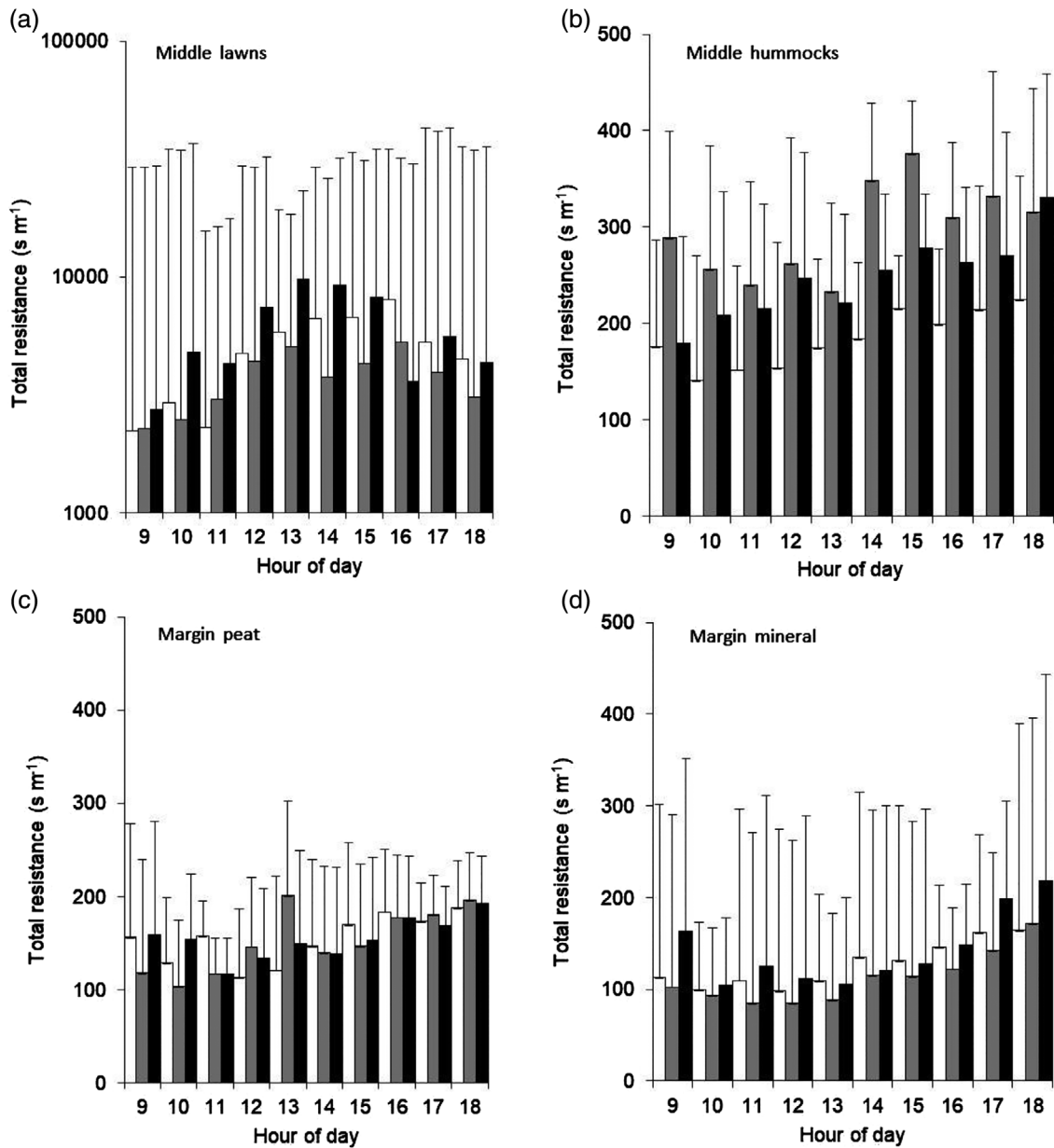


FIGURE 2 Temporal variation in median hourly (9:00 to 18:00) total resistance to evapotranspiration through the four defined zones between day of year 136 and 225 (May 15th and August 12th) 2012. Middle and margin determined by the distance to the pre-fire peatland–upland interface and the burn severity; higher burn severity within the margin peat. Middle further classified into hummocks (*Sphagnum fuscum*) and lawns (feather moss). Margin divided between areas that severely burned to mineral soil or areas in which a peat layer remained. Each colour represents a separate chamber within each zone; chamber 1, 2 and 3 are white, grey and black, respectively. Error bars represent quartile range. Note difference in scale and log scale of (a) compared to other plots

$$E = \frac{(\rho_{vs}^* - \rho_{vs})}{r_s} \quad (5)$$

We rearrange Equation (5) and solved for ρ_{vs} and subsequent rearrange Equation (3) and solving for e_c .

3 | RESULTS

3.1 | Spatiotemporal variation in r_{total}

There was a significant effect of measurement zone on median daytime (09:00–18:00) r_{total} . Median daytime r_{total} for the study period was orders of magnitude higher within the middle lawn (4610 ± 1380 s m⁻¹; median ± SD) than in the middle hummock (242 ± 52 s m⁻¹; t = 17.9, p < 0.0001), margin peat (155 ± s m⁻¹; t = 16.6, p < 0.0001) and margin mineral (132 ± 15 s m⁻¹; t = 16.7, p < 0.0001). Diurnal variations in r_{total} show consistent patterns

between chambers within each zone (Figure 2). Within the middle lawns, average r_{total} increases between 9:00 and 13:00. The resistance subsequently remains relatively consistent for the remainder of the day. There is considerable scatter around these median values. The high scatter in the middle lawn compared to other measurement regions likely results from the low ET used to calculate r_{total} and the resultant increased percentage error in measured ET. In comparison, the three other zones show a constant, or declining, median r_{total} during the first part of the day (9:00–12:00). Median r_{total} subsequently increases linearly with time through the remainder of the day (12:00 and 18:00).

Over the course of the growing season, r_{total} does not show a clear long-term trend within any measurement zone. However, moderate but consistent patterns in median daytime r_{total} are observed within each of the different zones during periods of high evaporative demand after rainfall, exemplified by the days 145–152 of drying that followed a rainfall on day of year 144 (Figure 3). Within the middle lawns, r_{total} triples over the first four days after rainfall, increasing

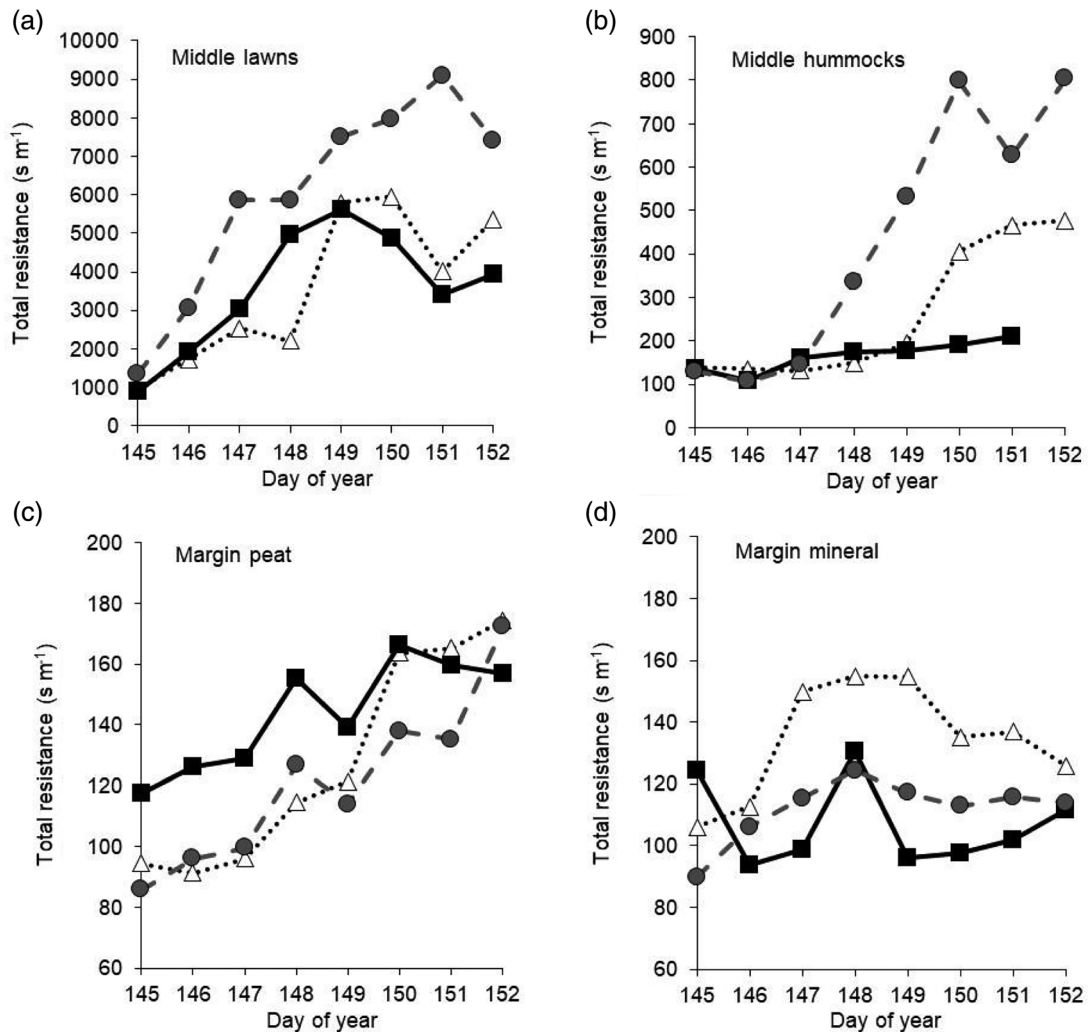


FIGURE 3 Daytime (09:00–18:00) median total resistance to evapotranspiration within each zone of the peatland for a 10 day rain free period that follows a rainfall event on day 144 (May 23rd). Each colour represents a different chamber within the defined zone; chamber 1, 2 and 3 are white, grey and black, respectively

from 1000 to 3000 s m⁻¹ (Figure 2a). The rate of increase in r_{total} subsequently reduces for the remainder of the rain free period. In comparison, r_{total} in the middle hummocks initially remains constant (Figure 2b). Four to six days after rainfall, on day of year 148 and 150, r_{total} subsequently increases for two of the chambers, with median daytime r_{total} increasing by 2.5–4.5 times its post rainfall values. The burned peat margin shows a consistent increase of ~50% in r_{total} for all three chambers during the dry period (Figure 2c) while r_{total} of the mineral margin remains constant through this period (Figure 2d).

3.2 | r_{total} versus tension at varying spatiotemporal scales

3.2.1 | Spatial variations

At the peatland scale, zones of high near-surface tension (middle lawns) correspond with high r_{total} (Figure 4a). Regions of low near-surface tension (middle hummocks and margins) correspond with low r_{total} . While there is a general pattern of increasing r_{total} with increasing soil tension, due to the clustering of resistance and tension measurements within burn severity classes, an empirical relationship is not clearly evident between near-surface tension and r_{total} at the peatlands scale. No relationship between r_{total} and water table depth is identifiable at the peatland scale (Figure 4b).

3.2.2 | Temporal variation; growing season

At each measurement location, a direct relationship between concurrent measurements of r_{total} and manual measurements of near-surface

tension across the growing season is not observed (data not shown). A very weak exponential relationship between concurrent near surface tension and r_{total} is evident between logging tensions and r_{total} within the single hummock ($R^2 = 0.13$, $n = 567$, $p < 0.001$; excluding $r_{total} > 500$ s m⁻¹ and measurements outside the time period 9:00–18:00). High scatter in the relationship may result from uncertainty in the humidity difference between the surface and atmosphere [the numerator within Equation (1)] resulting from small-scale spatial variability in surface temperatures. Within the 0.2 m² chambers, standard deviations in surface temperature within individual IR images ranges between 0.4 and 7°C ($\mu = 2.3$ °C, $n = 36$). The standard deviation is temperature dependent, with higher standard deviations observed at higher average temperatures ($R^2 = 0.52$, $p < 0.001$, $n = 36$). At 20°C, a 2°C error in the average surface temperature equates to additive errors in the calculated humidity difference of Equation (1) of 0.0031 kg m³ K⁻¹ due to errors in the calculation of ρ^*_{vs} (Oke, 1987). Excluding measurements below a threshold humidity difference of 0.01 kg m³ and also excluding low ET measurements (<0.2 mm h⁻¹) where percentage errors will be high, increases the strength of the relationship between r_{total} and near surface tension (Figure 5b, $R^2 = 0.34$, $p < 0.001$, $n = 375$). This relationship is principally driven by a nine day period with high evaporation gradients between DOY 186 and 196 (Figure 5a). This was the only period during the two month installation of the logging tensiometers when tensions exceeded 200 cm on successive days and reached a high of 250 cm (Figure 5a). During this nine day period, a strong exponential relationship is evident between tensions and r_{total} ($R^2 = 0.82$, $n = 89$, $p < 0.001$, Figure 5c). Under low positive tensions, r_{total} approximates values observed under laboratory conditions at similar tensions. However the gradient of the relationship between r_{total} and near surface tension is higher in the field conditions than under steady state laboratory conditions; higher r_{total} is observed in the field for a given near surface tension within the peat (Figure 5c).

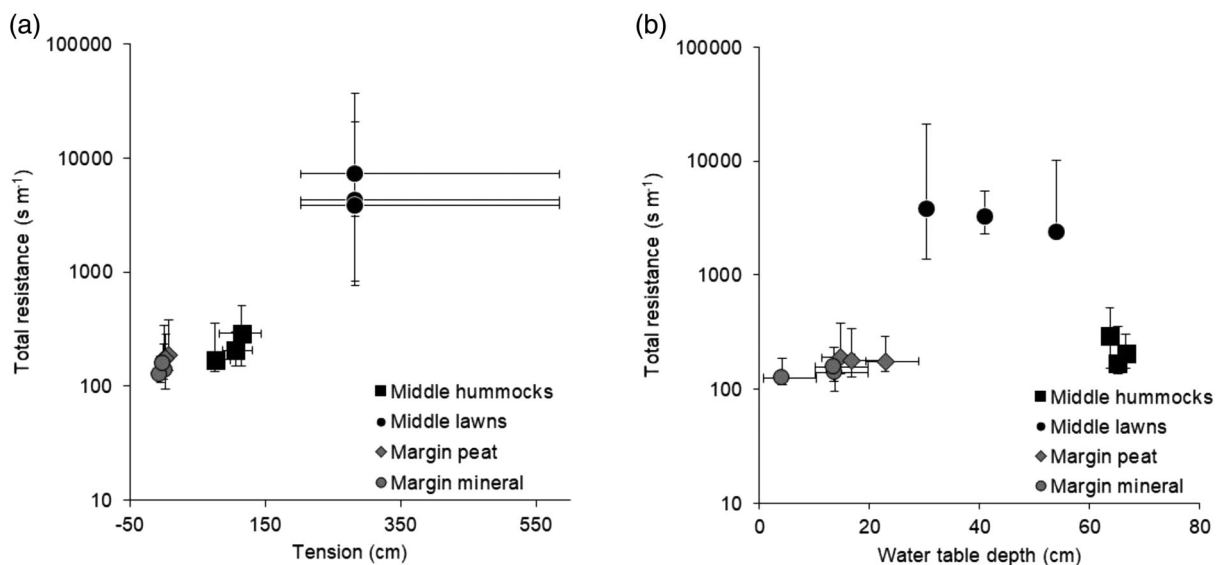


FIGURE 4 Median total resistance to evaporation and (a) median near-surface (5 cm depth) tension and (b) water table depth between day of year 136 and 225 (May 15th and August 12th) 2012. Error bars represent quartile range

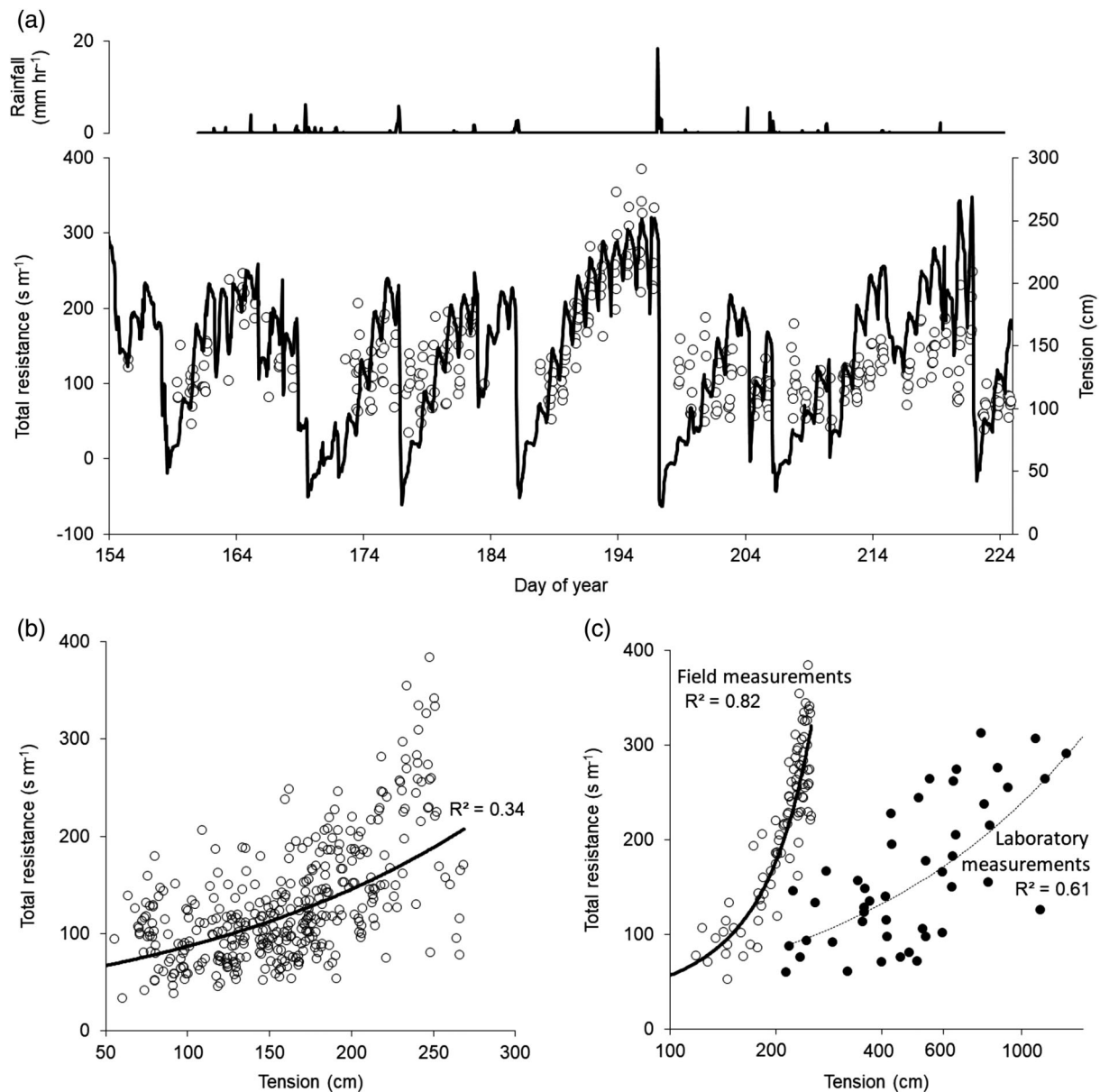


FIGURE 5 Relationship between near-surface (5 cm depth) tension and total resistance to ET in a single middle hummock (hummock chamber 2). (a) Top pane: Hourly precipitation. (a) Lower pane: Solid black line shows measured tension logged every 20 min. White circles show measured total resistance to ET where ET exceeds 0.2 mm h^{-1} and the humidity difference between the soil surface and atmosphere exceeds 0.01 kg m^{-3} . (b) Correlation between near-surface tension and total resistance over the entire time period presented in panel (a). (c) Open symbols: correlation between near-surface tension and total resistance during 10-day period between day 186 and 196 (July 4th and July 14th) in panel. Solid symbols, correlation between near-surface tension and total resistance observed under steady state laboratory conditions by Kettridge and Waddington (2014)

3.2.3 | Temporal variation: diurnal

The near-surface tension of the middle hummock shows a clear but moderate diurnal variation. The average tension for a given hour of the day ranges from a maximum of 159 cm at 19:00 to a minimum of 122 cm at 11:00. The median r_{total} for given hour of the day within the middle hummocks relates with the associated average tensions between 09:00 and 18:00 for each of the three chambers (Figure 6; $R^2 = 0.87, 0.71$ and 0.42 for chambers 1, 2 and

3, respectively). In comparison, within the middle lawns, the inverse relationship is observed. Over the extent of the study period, r_{total} peaked at 13:00 (Figure 7a), while near-surface tensions measured over the intense 24 h measurement period (normalized between their maximum and minimum values) peak at 00:00 and reach their minimum values at 12:00. In the margin zones, no diurnal variation is observed in near-surface tensions during the intensive 24 h study period (data not shown) despite diurnal variations in margin r_{total} (Figure 2c,d).

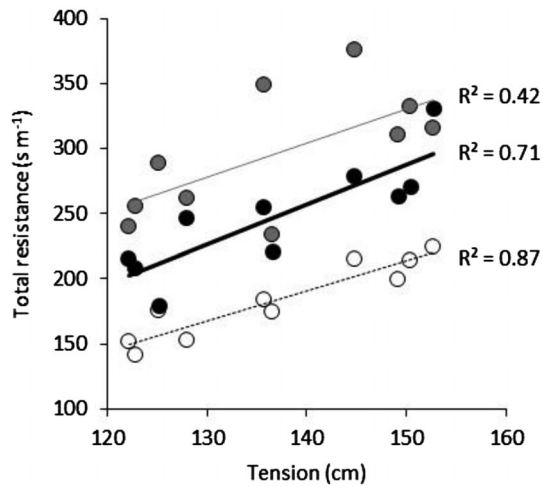


FIGURE 6 Regression analysis between hourly average near-surface tension (surface resistance measure at the same time each day average across days) and median total resistance to evapotranspiration within each of the middle *Sphagnum* hummocks; chamber 1, 2 and 3 indicated by white, grey and black symbols, respectively, over the period from day 154 to 225 (June 2nd to August 12th) 2012, see Figure 5. Each point represents a given hour of the day between 09:00 and 18:00 inclusive. Solid and dotted lines represent linear regression analysis

3.2.4 | Spatiotemporal variation in e_c

Within the middle hummock, $\log(e_c)$, equal to $\varphi_g \cdot \delta_s$, varies between 3.9 and 4.0 (Figure 8) and is at the upper end of the previously parameterised value that assumes near-surface moisture content of the peat is depleted. $\log(e_c)$ is significantly higher within the margin peat ($t = 8.4$, $p < 0.001$) and the margin mineral ($t = 7.5$, $p < 0.001$) than the middle hummock, with median $\log(e_c)$ ranging between 4.4 and 5.0. Within the middle lawn, $\log(e_c)$ extends further beyond the defined limits of past model parameterisations, with median values equal to 5.5–5.6. Within all zones, the interquartile range of $\log(e_c)$ is less than 0.9. Assuming the maximum δ_s equal to 2, minimum δ_s varies between just 1.7 and 1.9 to represent the observed interquartile range in $\log(e_c)$. The logging tensiometer provides a more continuous record of $\log(e_c)$ within the middle hummock. This demonstrates limited daytime variation in $\log(e_c)$ (Figure 9a). This daytime variability in $\log(e_c)$ is broadly equivalent to the multi-day range (Figure 9b). Between day of year 154 and 216, $\log(e_c)$ does fluctuate between 3.5 and 4.0. However, the direct relation between with periods of wetting and drying in response to rainfall is not clearly apparent.

4 | DISCUSSION

4.1 | Vertical hydraulic connectivity and its control on r_{total} dynamics

The magnitude, diurnal fluctuation and the short-term response to drying of r_{total} varies between peatland zones and likely results from

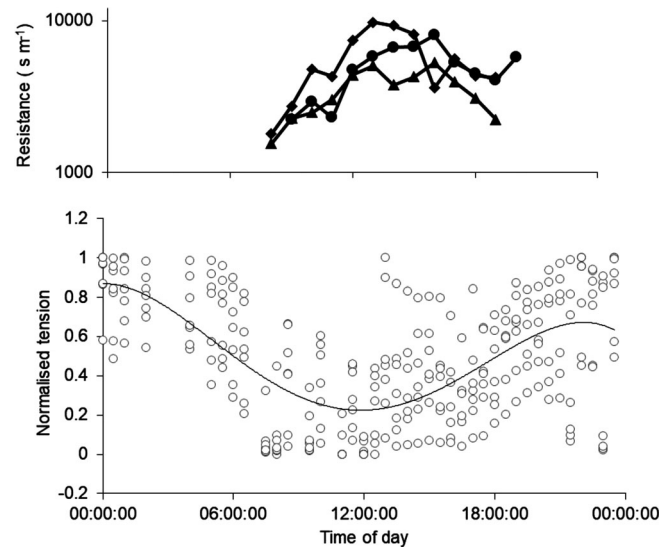


FIGURE 7 (a) Average hourly total resistance to evaporation from the three chambers installed within the middle lawns between day of year 136 and 225 (May 15th and August 12th) 2012. (b) Open symbols, normalized tension measured over a single 24-h period (intensive sampling) between 13:00 on day of year 164 to 13:00 on day of year 165, 2012 within seven separate tensiometers installed at a depth of 5 cm within the middle lawns (lower values indicative of wetter peat). Tensions measured approximately half hourly over a 24 h period. Tensions from each tensiometer are standardized between the minimum (zero) and maximum (one) tensions measured during the 24-h cycle. Solid line represents a 4th order polynomial fitted to the normalized ($R^2 = 0.39$, $p < 0.01$)

difference in the hydraulic connectives between the surface and the saturated peat below (McCarter & Price, 2014). Within the peatland margin burned to mineral soil (mineral margin), the sand profile with comparatively high water retentions, high unsaturated hydraulic conductivities (Carsel & Parrish, 1988; Smerdon et al., 2007) and shallow water table depths (Lukenbach et al., 2016) provides a well-connected system in which water can be supplied to the evaporating surface continuously through periods of high demand. At the other extreme, the middle lawns are highly disconnected vertically to the atmosphere (Lukenbach et al., 2016) as a result of the water repellent layer on sined feather moss (Kettridge & Waddington, 2014) and a deeper water table position. r_{total} increases quickly in response to drying because the supply of water to the peat surface is severely limited. The middle *Sphagnum* hummocks and margin peat fall between these two extremes. After a period of rainfall, the resistance of the middle hummocks initially remains low because of the high capacity for vertical water transport under unsaturated conditions (McCarter & Price, 2014). The subsequent divergence in the response is likely associated with differences in the burn severity of the hummocks. r_{total} increased to $>700 \text{ s m}^{-1}$ in a hummock that was more severely burned, with the removal of the *Sphagnum* capitula and the likely reduction in the connectivity (Lukenbach, Devito, et al., 2015). In comparison, the other two *Sphagnum* hummocks appeared visually unaffected by the fire and were better able to supply water to support

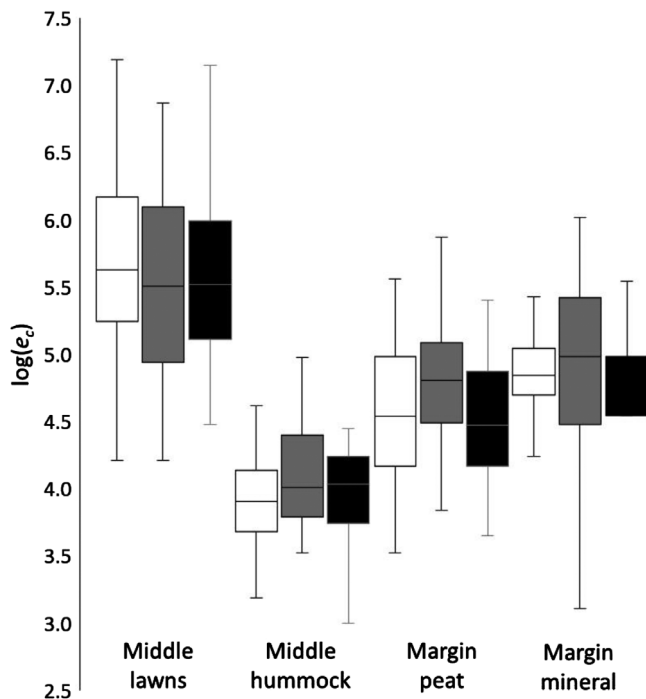


FIGURE 8 $\log(e_c)$ across the four different zones of the peatland between day of year 136 and 225 (May 15th and August 12th) 2012 from manual tensiometer measurements and concurrent chamber measurement. White, grey black represent chamber 1, 2 and 3 within each zone, respectively

evaporative demand. The margin peat showed a moderate capability to supply water to the remaining burned peat surface, with tension increasing consistently during the period of drying.

With evaporation being predominantly from the peat surface (Price et al., 2009), the lag of near-surface tensions to r_{total} provide an indication of the connectivity within the top peat layer. This lag differs between peatland zones, highlighting differences in the vertical connectivity. Diurnal variations in near-surface tensions within the middle *Sphagnum* hummocks correlate with average resistances showing a strong vertical connectivity; tensions at a depth of 0.05 m are closely in sync with surface tension. In comparison, the decrease in near-surface tension during the day in the middle feather moss lawns with no vascular vegetation while r_{total} increases suggest that near-surface tensions are lagged behind and poorly connected to the surface. Either that or: (1) the disconnect between the ceramic cup and the dry hydrophobic peat limits the response rate of the tensiometers, or (2) changes in the temperature of the tensiometer head space are strongly modifying tension readings (Butters & Cardon, 1998; Warrick et al., 1998). The measurement of near surface tensions within peat soils represents a core measurement challenge, with the open structure of the peat limiting contact between the peat and the tensiometers, tensiometers require larger ceramics to maintain contact preventing finer scale measurements within the top centimeter of the peat profile. More novel approaches to the quantification/characterize of the soil tensions and hydrological dynamics in the very near

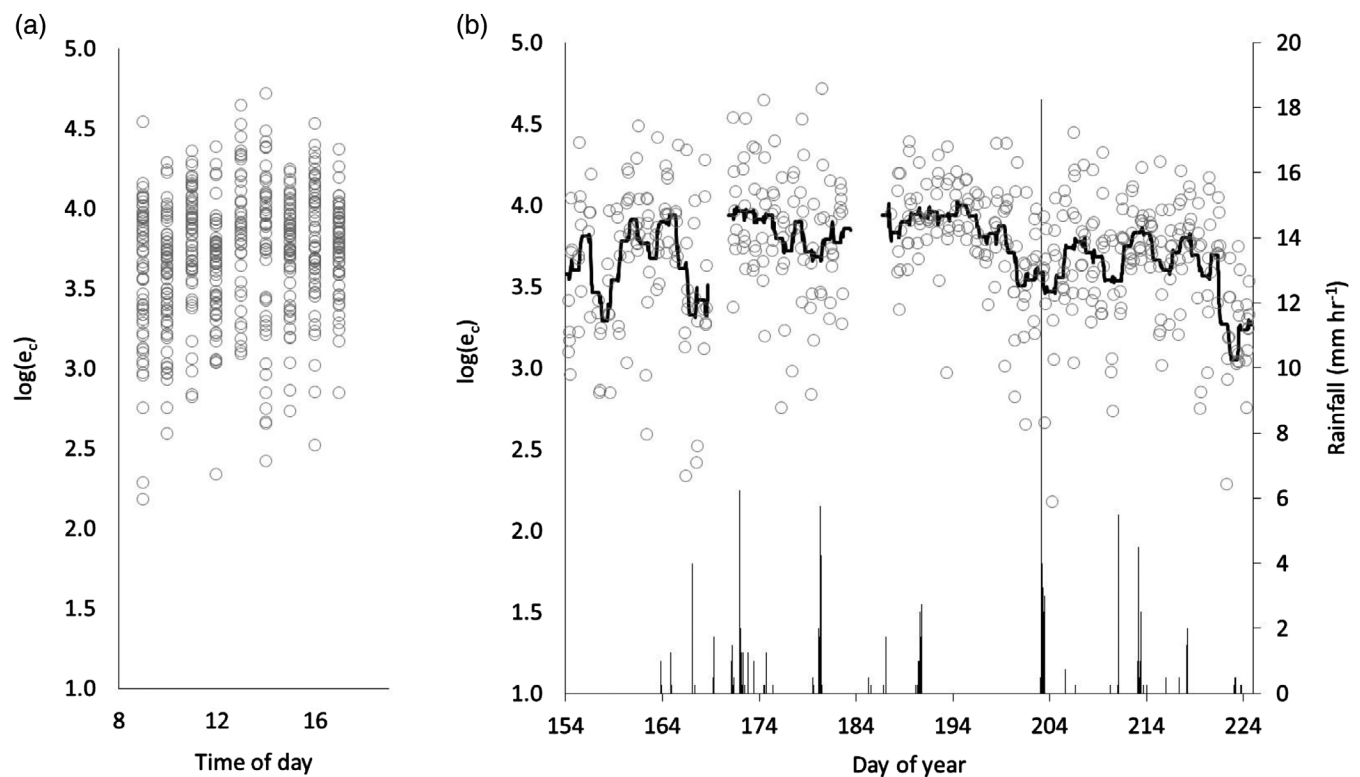


FIGURE 9 (a) Daytime variation in $\log(e_c)$ between 09:00 and 18:00 within middle hummock 2 between day of year 154 and 225. (b) Time series of selected data period. Solid lines represent a 48-h running mean of $\log(e_c)$ and hourly rainfall measured at the study site

surface of this open structure will likely support understanding of the regulation of water loss from these peat systems.

The lack of diurnal variation in the near-surface tension within the margin peat zone, largely as a result of the water table being in close proximity to the peat surface, suggests that observed variations in near-surface tensions result solely from diurnal fluctuations in tensions within the very near-surface of the remaining peat profile or a driven by the comparatively small transpiration component of ET. The nature of the connectivity between near-surface soil tension and surface peat vapour density therefore, represents an important control on evaporation that needs to be both effectively conceptualized and parameterised within hydrological models. To effectively parameterise these reductions in evaporation in response to periods of drying, but also understand how these near-surface peat soils are modified by burning, is therefore key. Although water repellent near-surface peat represents the most extreme (but not unusual) level of modification, it is also important to parameterise the full spectrum of wildfire induced hydrological changes that modify the response of evaporation to drying.

4.2 | The control of near-surface tension on evaporation

As hypothesized, at the peatland scale, increases in soil tension between zones of the peatland are associated with increases in r_{total} . However, despite the controlled nature of this field research, with concurrent measurement of r_{total} and near-surface tension, direct relationships between r_{total} and near-surface tension were not identifiable across the measurement locations. Here, we consider the extent to which: (a) tensions vary sufficiently over time at individual measurement locations to limit ET, (b) the uncertainty in individual r_{total} measurements, and (c) the disequilibrium between surface and subsurface tensions within the dynamic surface boundary under field conditions.

Errors in individual measurements of r_{total} are important to consider. These errors result from uncertainty in the humidity difference between the soil and atmosphere and in the measured ET. Errors in the calculated surface humidity of up to $\pm 0.003 \text{ kg m}^{-3}$ result from variability in measured surface temperatures. Within middle hummocks and margin areas, average humidity differences range between 0.008 and 0.02 kg m^{-3} at 13:00. Spatial variability in the surface temperature therefore results in errors in the humidity gradients of between 15%–38% for the different chambers. Thus, the direct comparison of individual measurements of r_{total} to near-surface tensions is unlikely to produce clear relationships when temporal variations in r_{total} are small. Further, despite the 40 manual measurements of tensions at each location through the study, periods of high tension were not captured. Within the margin peat and mineral zones, near-surface tensions remained within $\pm 0.05 \text{ m}$ of hydrostatic equilibrium for the entire study period (Lukenbach et al., 2016). No variation in r_{total} would thus be expected based on laboratory-derived relationships (cf. Kettridge & Waddington, 2014). Furthermore, the 90th percentile of measured tension is 154 cm within the middle hummock zone.

Similarly, the expected range in r_{total} from laboratory measurements equates to 85 s m^{-1} . While such a range in r_{total} is difficult to measure under field conditions, it is important in terms of water loss from the Boreal Plain landscape where small modifications in r_{total} can have important consequences for water conservation within these water limited environments (Devito et al., 2017). Such difficulties can be overcome by targeting periods of high evaporation and humidity gradients when percentage errors are small.

A weak relationship between r_{total} and near-surface tension was observed within the *Sphagnum* hummock; the high number of tensiometer measurements enabled both a larger range in near-surface tension to be observed and the exclusion of r_{total} measurements when errors were likely high. The relationship is dominated by a 10-day period of high ET, high humidity differences, and near-surface tensions which exceed 200 cm. During the remainder of the periods, r_{total} remains low and is poorly correlated to near-surface tensions. This switching between a low and a high resistance condition that depends on near-surface tension is consistent with laboratory-based observations (Kettridge & Waddington, 2014) and is analogous to the stage 1 and stage 2 evaporation (Lehmann et al., 2008) where high relative constant evaporation (stage 1) transitions to lower rate of evaporation (stage 2) that is controlled by vapour diffusion through the porous media. However, the reason for the period of strong relationship is unclear. While this period does represent the highest observed tensions during the study period, the enhanced relationship between near-surface tensions and r_{total} is observed prior to these high tensions being reached. Early during this period, tensions are comparable to times where little if any relationship is observable between near-surface tensions and r_{total} . In addition, ET is equally composed of transpiration and evaporation within this given hummock, and the observed increases in resistance may also result from a restriction in transpiration. During the period of strong relationship, the relationship observed between r_{total} and near-surface tension under dynamic field conditions is more sensitive compared to steady state laboratory conditions; with r_{total} increasing to higher values under a dynamic evaporative demand for a given near surface tension. This is indicative of the dynamic nature of the field measurements, with tensions at a depth of 0.05 m being in disequilibrium with the evaporative demand. Therefore, measured tensions in the near-surface are lower for a given r_{total} .

An approach to embed the connection between near-surface tension and vapour density within the Penman–Monteith equation has been proposed (Kellner, 2001). However, it is clear that this relationship must be directly parameterised for a given soil profile in a manner similar to any identified relationships between near surface tension and surface resistance. δ_s appears to not be impacted by precipitation inputs compared to laboratory parameterizations under steady state conditions, but with some variability associated with diurnal evaporation demand. High ET demand and low storage within the near surface may minimize periods of lower δ_s under field conditions. While this insensitivity is beneficial for model parameterisations, φ_g differs by orders of magnitude between the different zones of the peatland. Measurements within the middle hummock zone are comparable to

both initial applications of this modelling approach (Kellner, 2001) and laboratory based parameterisations (Kettridge & Waddington, 2014). However, φ_g is substantially greater within the margin zones and middle lawns. As a result of this variability, it is uncertain as to whether this approach provides any added benefit beyond empirical relationships between surface resistance and near-surface tensions.

4.3 | Moving forwards in peatland evaporation simulation

Within peatland hydrological models it is important to recognize that controls on evaporation go beyond water table depth. Effective simulations should acknowledge the important influence peat properties and water repellency can have on spatiotemporal evaporation dynamics. But in these more advanced models that incorporate aspects of vadose zone hydrology, near-surface field based measurements cannot directly quantify surface controls on evaporation without further measurement advances. This does not on its own indicate that laboratory derived parameterizations under pseudo steady-state laboratory conditions will not effectively support the development of peatland hydrological models. Simulated surface tensions can vary substantially within the top 5 cm of the peat profile (McCarter & Price, 2014). The strength and dynamic nature of this near-surface tension gradient may underlie the disconnect between field measurements of surface resistance and near surface tension. Moving forward, simulating the vadose zone hydrology of soil profiles of known hydrophysical properties and driven by measured rates of evaporation would offer the opportunity to infer the relationship between evaporation and resultant simulated surface and near surface tension. While this does not independently derive this critical relationship, such an inverse modelling approach would generate surface resistance-tension relationships that can be evaluated again using those obtained under laboratory and field based conditions, offering a strong opportunity for moving forward.

Alternatively, additional approaches formulated from first principles could offer future promise in representing peatland evaporation. Clear threshold responses, switching between high and low rates of evaporation, have been observed in peat profiles under laboratory conditions (Kettridge & Waddington, 2014), with some evidence of such a response under field conditions within this study that is representative of a transition between stage 1 and 2 evaporation. As a result, the application of evaporation lengths and quantification of this transition may provide a very compelling future approach within peatland ecosystems (Or et al., 2013). To date the application of evaporation lengths has targeted mineral soils using differences in soil types over regional and even global scales (Lehmann et al., 2018) to explore spatiotemporal variations in the evaporation feedback response. The diversity of water retention within peat soils over the decimetre scale explored here transcends much of this diversity in soil properties, in the peat soils themselves (from moss surface to decomposed exposed peat where peat soils still persist, Thompson &

Waddington, 2013) to sandy and clay rich mineral soils exposed by complete combustion of the overlaying peat. However, traditional and widely applied modelling software can be fairly restrictive in the application of dynamic surface resistance values (e.g., Hydrus) and therefore can perpetuate the application of a simple threshold response (Kettridge et al., 2016; McCarter & Price, 2014), that does not reflect the more complex dynamics observed.

5 | CONCLUSIONS

This work illustrates the challenges of accurately incorporating the response of evaporation to peatland drying into numerical modelling frameworks, even when the water table remains comparatively close to the peatland surface. The surface resistance in this study was shown to be neither constant in space nor time, with differences likely meaningfully impacting the ecohydrological response of peatland ecosystems post disturbance. We have shown that the controls occur in the very near-surface, making them difficult if not impossible to measure with traditional field based instrumentation. Laboratory based measurements under steady state conditions (Bond-Lamberty et al., 2011; Kettridge & Waddington, 2014) offer a starting point to parameterise the control of surface tensions on the surface resistance. However, we have shown that modifications are necessary to apply such relationships to the range of conditions observed across field sites. Dynamic conditions are shown here to result in differences in the relationship between measurable near-surface tensions and surface resistances. We suggest that the gradient in soil tensions in the near-surface peat is enhanced under non steady state evaporation conditions observed under field conditions, resulting in an apparent insensitivity of r_{total} to variations in near-surface tension. But the connectivity between r_{total} and near-surface tensions also shows an apparent temporal switching on and off, turning on for a discrete dry period of time after rainfall. Threshold responses therefore appear to underlie this relationship, occurring only during the highest rates of evaporation observed in a given year; although this likely differs between peatlands and climates, notably future climates.

ACKNOWLEDGEMENTS

Financial support was provided by Syncrude Canada Ltd, Canadian Natural Resources Ltd. (SCL4600100599) industry partners and Natural Sciences and Engineering Research Council–Collaborative Research and Development grant (NSERC-CRDPJ477235-14) of Canada to KJD. We thank two anonymous reviewers for their feedback on an earlier version of the manuscript.

DATA AVAILABILITY STATEMENT

The data that support the findings of this study are available from the corresponding author upon reasonable request.

ORCID

Nicholas Kettridge  <https://orcid.org/0000-0003-3995-0305>

Kevin J. Devito  <https://orcid.org/0000-0002-8216-0985>

Carl A. Mendoza  <https://orcid.org/0000-0002-2731-0004>

REFERENCES

- Admiral, S. W., & Lafleur, P. M. (2007). Modelling of latent heat partitioning at a bog peatland. *Agricultural and Forest Meteorology*, *144*, 213–229.
- Alvenäs, G., & Jansson, P. E. (1997). Model for evaporation, moisture and temperature of bare soil: Calibration and sensitivity analysis. *Agricultural and Forest Meteorology*, *88*, 47–56.
- Belyea, L. R., & Baird, A. J. (2006). Beyond “the limits to peat bog growth”: Cross-scale feedback in peatland development. *Ecological Monographs*, *76*, 299–322.
- Bond-Lamberty, B., Gower, S. T., Amiro, B., & Ewers, B. E. (2011). Measurement and modelling of bryophyte evaporation in a boreal forest chronosequence. *Ecohydrology*, *4*, 26–35.
- Bond-Lamberty, B., Peckham, S. D., Gower, S. T., & Ewers, B. E. (2009). Effects of fire on regional evapotranspiration in the central Canadian boreal forest. *Global Change Biology*, *15*, 1242–1254.
- Brown, S. M., Petrone, R. M., Chasmer, L., Mendoza, C., Lazerjan, M. S., Landhausser, S., Silins, U., & Devito, K. J. (2014). The influence of rooting zone soil moisture on evapotranspiration from above and within a Western Boreal Plain aspen forest. *Hydrological Processes*, *28*, 4449–4462.
- Brown, S. M., Petrone, R. M., Mendoza, C., & Devito, K. J. (2010). Surface vegetation controls on evapotranspiration from a sub-humid Western Boreal Plain wetland. *Hydrological Processes*, *24*, 1072–1085.
- Butters, G. L., & Cardon, G. E. (1998). Temperature effects on air-pocket tensiometers. *Soil Science*, *163*, 677–685.
- Carsel, R. F., & Parrish, R. S. (1988). Developing joint probability distributions of soil water retention characteristics. *Water Resources Research*, *24*, 755–769.
- Devito, K. J., Hokanson, K. J., Moore, P. A., Kettridge, N., Anderson, A. E., Chasmer, L., Hopkinson, C., Lukenbach, M. C., Mendoza, C. A., Morissette, J., & Peters, D. L. (2017). Landscape controls on long-term runoff in subhumid heterogeneous Boreal Plains catchments. *Hydrological Processes*, *31*(15), 2737–2751.
- Devito, K., Mendoza, C., & Qualizza, C. (2012). *Conceptualizing water movement in the Boreal Plains. Implications for watershed reconstruction*. Synthesis report prepared for the Canadian Oil Sands Network for research and development, Environmental and Reclamation Research Group, p. 164.
- Gibson, J. J., Birks, S. J., Kumar, S., McEachern, P. M., & Hazewinkel, R. (2010). Inter-annual variations in water yield to lakes in northeastern Alberta: Implications for estimating critical loads of acidity. *Journal of Limnology*, *69*, 126–134.
- Helbig, M., Waddington, J. M., Alekseychik, P., Amiro, B., Aurela, M., Barr, A. G., Black, T. A., Blanken, P. D., Carey, S. K., Chen, J., Chi, J., Desai, A. R., Dunn, A., Euskirchen, E., Friborg, T., Flanagan, L. B., Forbrich, I., Grelle, A., Harder, S., ... Zyryanov, V. (2020). Increasing contribution of peatlands to boreal evapotranspiration in a warming climate. *Nature Climate Change*, *10*, 555–560.
- Hokanson, K. J., Mendoza, C. A., & Devito, K. J. (2019). Interactions Between regional climate, surficial geology, and topography: Characterizing shallow groundwater systems in sub-humid, low-relief landscapes. *Water Resources Research*, *55*, 284–297.
- Hokanson, K. J., Peterson, E. S., Devito, K. J., & Mendoza, C. A. (2020). Forestland-peatland hydrologic connectivity in water-limited environments: Hydraulic gradients often oppose topography. *Environmental Research Letters*, *15*, 034021.
- Holden, J. (2005). Peatland hydrology and carbon cycling: Why small-scale process matters. *Philosophical Transactions of the Royal Society*, *363*, 2891–2913.
- Kellner, E. (2001). *Surface energy exchange and hydrology of a poor Sphagnum mire* (PhD thesis). Uppsaliensis, Sweden: ACTA Universitatis Uppsaliensis.
- Kettridge, N., & Baird, A. (2008). Modelling soil temperatures in northern peatlands. *European Journal of Soil Science*, *59*, 327–338.
- Kettridge, N., Lukenbach, M. C., Hokanson, K., Hopkinson, C., Devito, K. J., Petrone, R. M., Mendoza, C. A., & Waddington, J. M. (2017). Low evaporation enhances the resilience of peatland carbon stocks to fire. *Geophysical Research Letters*, *44*, 9341–9349.
- Kettridge, N., Lukenbach, M. C., Hokanson, K. J., Devito, K. J., Petrone, R. M., Mendoza, C. A., & Waddington, J. M. (2019). Severe wildfire exposes remnant peat carbon stocks to increased post-fire drying. *Scientific Reports*, *9*, 1–6.
- Kettridge, N., Thompson, D. K., Bombonato, L., Turetsky, M. R., Benscotter, B. W., & Waddington, J. M. (2013). The ecohydrology of forested peatlands: Simulating the effects of tree shading on moss evaporation and species composition. *Journal of Geophysical Research: Biogeosciences*, *118*, 422–435.
- Kettridge, N., Tilak, A. S., Devito, K. J., Petrone, R. M., Mendoza, C. A., & Waddington, J. M. (2016). Moss and peat hydraulic properties are optimized to maximize peatland water use efficiency. *Ecohydrology*, *9*, 1039–1051.
- Kettridge, N., Turetsky, M. R., Sherwood, J. H., Thompson, D. K., Miller, C. A., Benscotter, B. W., Flannigan, M. D., Wotton, B. M., & Waddington, J. M. (2015). Moderate drop in water table increases peatland vulnerability to post-fire regime shift. *Scientific Reports*, *5*, 8063.
- Kettridge, N., & Waddington, J. M. (2014). Towards quantifying the negative feedback regulation of peatland evaporation to drought. *Hydrological Processes*, *28*, 3728–3740.
- Lehmann, P., Assouline, S., & Or, D. (2008). Characteristic lengths affecting evaporative drying of porous media. *Physical Review E*, *77* (5), 056309.
- Lehmann, P., Merlin, O., Gentine, P., & Or, D. (2018). Soil texture effects on surface resistance to bare-soil evaporation. *Geophysical Research Letters*, *45*, 10–398.
- Lukenbach, M. C., Devito, K. J., Kettridge, N., Petrone, R. M., & Waddington, J. M. (2015). Hydrogeological controls on post-fire moss recovery in peatlands. *Journal of Hydrology*, *530*, 405–418.
- Lukenbach, M. C., Devito, K. J., Kettridge, N., Petrone, R. M., & Waddington, J. M. (2016). Burn severity alters peatland moss water availability: Implications for post-fire recovery. *Ecohydrology*, *9*, 341–353.
- Lukenbach, M. C., Hokanson, K. J., Moore, P. A., Devito, K. J., Kettridge, N., Thompson, D. K., Wotton, B. M., Petrone, R. M., & Waddington, J. M. (2015). Hydrological controls on deep burning in a northern forested peatland. *Hydrological Processes*, *29*, 4114–4124.
- McCarter, C. P., & Price, J. S. (2014). Ecohydrology of *Sphagnum* moss hummocks: Mechanisms of capitula water supply and simulated effects of evaporation. *Ecohydrology*, *7*, 33–44.
- McLeod, M. K., Daniel, H., Faulkner, R., & Murison, R. (2004). Evaluation of an enclosed portable chamber to measure crop and pasture actual evapotranspiration at small scale. *Agricultural Water Management*, *67*, 15–34.
- Moore, P. A., Lukenbach, M. C., Kettridge, N., Petrone, R. M., Devito, K. D., & Waddington, J. M. (2017). Peatland water repellency: Importance of soil water content, moss species, and burn severity. *Journal of Hydrology*, *554*, 656–665.
- Moore, P. A., & Waddington, J. M. (2015). Modelling *Sphagnum* moisture stress in response to 21st century climate change. *Hydrological Processes*, *29*, 3966–3982.
- Morison, M., Petrone, R. M., Wilkinson, S. L., Green, A., & Waddington, J. M. (2019). Ecosystem scale evapotranspiration and CO₂ exchange in a burned and unburned peatland: Implications for the ecohydrological resilience of carbon stocks to wildfire. *Ecohydrology*, *13*, e2189.
- Nijp, J. J., Metselaar, K., Limpens, J., Teutschbein, C., Peichl, M., Nilsson, M. B., Berendse, F., & van der Zee, S. E. (2017). Including hydrological self-regulating processes in peatland models: Effects on

- peatmoss drought projections. *Science of the Total Environment*, 580, 1389–1400.
- Oke, T. R. (1987). *Boundary layer climates*. Routledge.
- Or, D., Lehmann, P., Shakraeni, E., & Shokri, N. (2013). Advances in soil evaporation physics—A review. *Vadose Zone Journal*, 12, 1–16.
- Petrone, R. M., Silins, U., & Devito, K. J. (2007). Dynamics of evapotranspiration from a riparian pond complex in the Western Boreal Forest, Alberta, Canada. *Hydrological Processes*, 21, 1391–1401.
- Philip, J. R. (1957). Evaporation, and moisture and heat fields in the soil. *Journal of Meteorology*, 14, 354–366.
- Plach, J. M., Petrone, R. M., Waddington, J. M., Kettridge, N., & Devito, K. J. (2016). Hydroclimatic influences on peatland CO₂ exchange following upland forest harvesting on the Boreal Plains. *Ecohydrology*, 9, 1590–1603.
- Price, J. S., Edwards, T. W., Yi, Y., & Whittington, P. N. (2009). Physical and isotopic characterization of evaporation from *Sphagnum* moss. *Journal of Hydrology*, 369, 175–182.
- Schneider, R. R., Devito, K. J., Kettridge, N., & Bayne, E. (2016). Moving beyond bioclimatic envelope models: Integrating upland forest and peatland processes to predict ecosystem transitions under climate change in the western Canadian boreal plain. *Ecohydrology*, 9, 899–908.
- Smerdon, B. D., Mendoza, C. A., & Devito, K. J. (2007). Simulations of fully coupled lake-groundwater exchange in a subhumid climate with an integrated hydrologic model. *Water Resources Research*, 43, W01416.
- Sonnentag, O., Chen, J. M., Roulet, N. T., Ju, W., & Govind, A. (2008). Spatially explicit simulation of peatland hydrology and carbon dioxide exchange: Influence of mesoscale topography. *Journal of Geophysical Research Biogeosciences*, 113, G02005.
- Strack, M., Waddington, J. M., & Tuittila, E. S. (2004). Effect of water table drawdown on northern peatland methane dynamics: Implications for climate change. *Global Biogeochemical Cycles*, 18, GB4003.
- Thompson, D. K., Bencotter, B. W., & Waddington, J. M. (2014). Water balance of a burned and unburned forested boreal peatland. *Hydrological Processes*, 28, 5954–5964.
- Thompson, D. K., & Waddington, J. M. (2013). Wildfire effects on vadose zone hydrology in forested boreal peatland microforms. *Journal of Hydrology*, 486, 48–56.
- Thompson, D. K., Wotton, B. M., & Waddington, J. M. (2015). Estimating the heat transfer to an organic soil surface during crown fire. *International Journal of Wildland Fire*, 24, 120–129.
- Turetsky, M., Wieder, K., Halsey, L., & Vitt, D. (2002). Current disturbance and the diminishing peatland carbon sink. *Geophysical Research Letters*, 29, 1526.
- Waddington, J. M., Morris, P. J., Kettridge, N., Granath, G., Thompson, D. K., & Moore, P. A. (2015). Hydrological feedbacks in northern peatlands. *Ecohydrology*, 8, 113–127.
- Warrick, A. W., Wierenga, P. J., Young, M. H., & Musil, S. A. (1998). Diurnal fluctuations of tensiometric readings due to surface temperature changes. *Water Resources Research*, 34, 2863–2869.
- Wilkinson, S. L., Verkaik, G., Moore, P. A., & Waddington, J. M. (2020). Threshold peat burn severity breaks evaporation-limiting feedback. *Ecohydrology*, 13, e2168.
- Yu, Z. C. (2012). Northern peatland carbon stocks and dynamics: A review. *Biogeosciences*, 9, 4071–4085.

SUPPORTING INFORMATION

Additional supporting information may be found online in the Supporting Information section at the end of this article.

How to cite this article: Kettridge N, Lukenbach MC, Hokanson KJ, et al. Regulation of peatland evaporation following wildfire; the complex control of soil tension under dynamic evaporation demand. *Hydrological Processes*. 2021;35: e14132. <https://doi.org/10.1002/hyp.14132>